

RESEARCH ARTICLE

An in vitro comparison of human corneal epithelial cell activity and inflammatory response on differently designed ocular amniotic membranes and a clinical case study

Yong Mao¹ | Nicole M. Protzman² | Nikita John¹ | Adam Kuehn³ |
 Desiree Long³ | Raja Sivalenka³ | Radoslaw A. Junka³ | Anish U. Shah⁴ |
 Anna Gosiewska³  | Robert J. Hariri³ | Stephen A. Brigido³

¹Department of Chemistry and Chemical Biology, Rutgers University Laboratory for Biomaterials Research, Piscataway, New Jersey, USA

²Department of Research, Healthcare Analytics, LLC, Easton, Pennsylvania, USA

³Celularity Inc., Florham Park, New Jersey, USA

⁴Department of Ophthalmology, Norwich Ophthalmology Group, Norwich, Connecticut, USA

Correspondence

Anna Gosiewska, Celularity Inc., 170 Park Ave., Florham Park, NJ 07932, USA.
 Email: anna.gosiewska@celularity.com

Funding information

Celularity Inc.; Laboratory for Biomaterials Research at Rutgers University

Abstract

Amniotic membrane (AM) is a naturally derived biomaterial with biological and mechanical properties important to Ophthalmology. The epithelial side of the AM promotes epithelialization, while the stromal side regulates inflammation. However, not all AMs are equal. AMs undergo different processing with resultant changes in cellular content and structure. This study evaluates the effects of sidedness and processing on human corneal epithelial cell (HCEC) activity, the effect of processing on HCEC inflammatory response, and then a case study is presented. Three differently processed, commercially available ocular AMs were selected: (1) Biovance[®]3L Ocular, a decellularized, dehydrated human AM (DDHAM), (2) AMBIO2[®], a dehydrated human AM (DHAM), and (3) AmnioGraft[®], a cryopreserved human AM (CHAM). HCECs were seeded onto the AMs and incubated for 1, 4 and 7 days. Cell adhesion and viability were evaluated using alamarBlue assay. HCEC migration was evaluated using a scratch wound assay. An inflammatory response was induced by TNF- α treatment. The effect of AM on the expression of pro-inflammatory genes in HCECs was compared using quantitative polymerase chain reaction (qPCR). Staining confirmed complete decellularization and the absence of nuclei in DDHAM. HCEC activity was best supported on the stromal side of DDHAM. Under inflammatory stimulation, DDHAM promoted a higher initial inflammatory response with a declining trend across time. Clinically, DDHAM was used to successfully treat anterior basement membrane dystrophy. Compared with DHAM and CHAM, DDHAM had significant positive effects on the cellular activities of HCECs in vitro, which may suggest greater ocular cell compatibility in vivo.

KEYWORDS

anterior basement membrane dystrophy, biomaterial, decellularized scaffold, human amniotic membrane, human ocular epithelial cells, ocular surface

This is an open access article under the terms of the [Creative Commons Attribution-NonCommercial-NoDerivs](https://creativecommons.org/licenses/by-nc-nd/4.0/) License, which permits use and distribution in any medium, provided the original work is properly cited, the use is non-commercial and no modifications or adaptations are made.

© 2022 Celularity and The Authors. *Journal of Biomedical Materials Research Part B: Applied Biomaterials* published by Wiley Periodicals LLC.

1 | INTRODUCTION

Amniotic membrane (AM) is a naturally derived biomaterial with unique biological and mechanical properties that render it particularly suitable for use in ophthalmology.¹⁻⁶ Amnion tissue is thought to promote healing and reconstruction of the ocular surface through the promotion of epithelialization,^{5,7-9} reduction of inflammation,¹⁰⁻¹² inhibition of scar tissue formation,¹³⁻¹⁵ blockage of new blood vessels,¹⁶ and the ability to act as an antimicrobial agent.¹⁷⁻²² In ophthalmology, the AM is widely used to treat a variety of ocular conditions. Clinically, the AM can be used as a surgical patch, as a substrate to replace damaged ocular tissue, or in combination as both a patch and a substrate.

As a patch, the AM acts as a temporary biological bandage or contact lens, promoting re-epithelialization of the host tissue beneath the patch^{3,5} and is placed stromal side down to downregulate the inflammatory response by trapping inflammatory cells and inducing apoptosis.^{23,24} By placing the AM epithelial side up, the AM acts as a substrate and scaffold for epithelial cell migration and growth.³ Although it is widely accepted that the AM should be placed epithelial side up to promote re-epithelialization,²⁵ the stromal side of the membrane^{7,8} has also been shown to support epithelial cell growth.²⁶ Notably, much of the existing research is limited to cryopreserved AMs, and it remains unclear whether these findings also apply to other AMs that have undergone different processing methodologies.

Prior to clinical application, the AM is sterilized and processed with resultant changes to cellular content and structure.^{1,27,28} This tissue can be used directly, or it can undergo the additional process of decellularization.²⁹ Decellularization is a process whereby endogenous cells, cell debris, and DNA remnants are removed to prevent an immune response, while retaining the natural structural and chemical elements of the extracellular matrix (ECM).³⁰ Previous studies have demonstrated a correlation between the quantity of residual DNA in ECM products and the host inflammatory response.^{31,32} As with the preservation of tissue, decellularization can also affect the structures and entities within the ECM.³³ Therefore, successful preservation-decellularization protocols must delicately balance the removal of cellular material and the retention of the innate properties and functional characteristics of ECM.^{30,33,34} To our knowledge, no studies have evaluated how differing preservation-decellularization protocols affect the cellular activity and inflammatory response of human corneal epithelial cells (HCECs).

For the first time, this project aims to evaluate:

1. the effect of AM sidedness (i.e., epithelial vs stromal) and processing methodology on the cellular activities of HCEC (i.e., adhesion, viability, and migration),
2. the effect of different processing methodologies on the inflammatory response of HCECs (i.e., expression of pro-inflammatory genes).

Therefore, three differently processed commercially available ocular AMs were used for comparison:

1. Biovance[®]3L Ocular (Celularity, Florham Park, NJ), a decellularized, dehydrated human amniotic membrane (DDHAM),

2. AMBIO2[®] (Katena, Parsippany, NJ), a dehydrated human amniotic membrane (DHAM),
3. AmnioGraft[®] (Biotissue, Miami, FL), a cryopreserved human amniotic membrane (CHAM).

Biovance[®]3L Ocular is a three-layer DDHAM. It is designed uniquely with the stromal side facing out. Therefore, the stromal side interfaces with the ocular surface regardless of its orientation. Furthermore, having three layers enhances its handling properties. The AM is excised from qualified term placentas, washed, and scraped to remove extraneous tissues and cells. The tissue is then decellularized using an osmotic shock followed by a mild detergent treatment, dried, and sterilized. Previous research has confirmed that this proprietary decellularization process removes residual cells, cell debris, growth factors, and cytokines, while retaining an ECM structure with high collagen content and key bioactive molecules, such as fibronectin, laminin, glycosaminoglycans, and elastin.³⁵

AMBIO2[®] is a single-layer, aseptically processed DHAM. The dehydration process removes moisture, while preserving the structural matrix and biological components of the tissue (Instructions for Use, 2021), including growth factors and cytokines.

AmnioGraft[®] is a single-layer CHAM. The AM is preserved using a proprietary cryopreservation method, CRYOTEK[®]. The cryopreservation process renders the amniotic epithelial cells nonviable, while maintaining an intact cellular structure and preserving growth factors and cytokines.³⁶

DDHAM retains its native ECM and is devoid of all cellular components, DNA, growth factors, and cytokines. Therefore, the authors hypothesize that DDHAM will provide a more cell-friendly matrix supporting the cellular activity and inflammatory response of HCECs compared with the two other ocular AMs containing residual DNA and other cellular components. Results from this *in vitro* study will further the basic understanding of how the preservation and decellularization of amnion tissue affects the activity of human ocular epithelial cells. It also has the potential to elucidate the clinical application of DDHAM to support corneal and conjunctival related injuries or defects, such as corneal epithelial defect healing, pterygium repair, fornix reconstruction, and other ocular procedures.

2 | MATERIALS AND METHODS

Since the testing materials are commercially available products and this study did not require direct interaction with human subjects (donors), institutional review board approval was not required.

2.1 | Ocular AMs

Three ocular AMs were used in this study: DDHAM, DHAM, and CHAM. DDHAM and DHAM samples were stored at room temperature. CHAM samples were stored at -80°C . All AMs were handled according to the manufacturer's instructions. DDHAM samples came as individually packaged 10 mm discs. Therefore, 10 mm discs were

made from DHAM sheet, using a 10 mm biopsy punch (Thermo Fisher Scientific, Waltham, MA, USA). Each piece (5 × 10 cm) of CHAM was thawed and washed in 20 ml of phosphate buffered saline (PBS) in a petri dish for 10 min (min) to remove the cryoprotectants and 10 mm discs were made from the washed AMs using 10 mm biopsy punch (Supplementary Figure 1). DDHAM is multilayered (three layered) with the stromal side of the AM facing out on both sides. To evaluate the sidedness of DDHAM, a differently designed version was prepared (three layered) with the epithelial side of the AM facing out on both sides, DDHAM (E). A 10 mm discs of each AM sample were placed in the wells of a 48-well plate (1 disc/well) (Cell-Repellent 48-Well Microplate, Greiner Bio-One, Monroe, NC, USA) with either the stromal side or the epithelial side of the AM in contact with the cells. A sterile O-ring (McMaster-Carr, Robbinsville, NJ, USA), measuring 2 mm in width with 7 mm inner diameter, was placed on top of each AM to hold the AM in place. Amniotic membranes were pre-conditioned with growth medium (0.4 ml/well) at 37°C for 2 h before they were seeded with cells. At least two lots (donors) of each type of AM were used in this study. In each independent experiment, four samples ($n = 4$) from each AM were used, of which two samples were from one lot and two samples were from another lot. At least two independent experiments were performed for each individual assay. Standard tissue culture treated plastic (TCP) was used as a positive control to ensure proper cell culturing (data not shown).

2.2 | Primary cells

The HCECs (Cat#PCS-700-010, Lot# 80915170), corneal epithelial cell base medium, and corneal epithelial cell growth kit were purchased from ATCC (Manassas, VA, USA). The complete growth medium for HCECs was prepared according to the manufacturer's instructions.

2.3 | Assessment of cell adhesion to AMs

Assessment of cell adhesion to AMs was performed in accordance with previous reports.³⁷ HCECs at passage 4 (P4) were cultured to 80% confluence in 10 cm cell culture dishes following the manufacturer's instructions. Cells were rinsed once with 5 ml phosphate-buffered saline (PBS)/dish. One milliliter of 0.25% trypsin (Thermo Fisher Scientific, Waltham, MA, USA) was added to each dish and incubated at 37°C for 5 min. Two milliliters of minimum essential medium-alpha (Thermo Fisher Scientific, Waltham, MA, USA), containing 10% fetal bovine serum (FBS) was added to the dish to neutralize the trypsin. Cells were transferred to 15 ml conical tubes and centrifuged at 1000 RPM (Revolutions Per Minute) for 5 min. Cells were re-suspended in complete growth medium and counted using a hemocytometer.

HCECs (2×10^4 /well) were added to each well containing the pre-conditioned AMs. The plates were incubated at 37°C with 5% CO₂ and 95% humidity. After incubation for 24 h, the media were removed, and the cells were washed once with PBS. The viability of adhered cells was detected using the alamarBlue assay. Briefly, 0.2 ml/well of alamarBlue

solution, consisting of complete growth medium +10% alamarBlue reagent (Bio-Rad, Hercules, CA, USA) was added to each well and incubated at 37°C for 45 min. After incubation, 0.1 ml/well of supernatant was transferred to a 96-well plate. Fluorescence intensity was measured using a multimode microplate reader (Spark[®], TECAN, Switzerland) at excitation/emission (Ex/Em) = 540 nm/590 nm. The fluorescence intensity was expressed in arbitrary units (AU). A preliminary experiment was conducted to evaluate the adhesion and spreading of HCECs. After incubation for 24 h, the proliferation of cells was minimal (data not shown), permitting cell adhesion to be monitored at this time point.

2.4 | Staining of AMs and cells

To visualize the structural features of AMs, three different AMs were rehydrated, washed, and embedded in Tissue-Tek O.C.T. compound (Sakura, Torrance, CA, USA) vertically. Five micron/slice cryosections were made using Leica CM1850 cryostat (Leica Biosystems, Buffalo Grove, IL, USA). The cryosections on microscope slides were fixed with 4% paraformaldehyde for 1 h and permeabilized in 0.5% Triton X100 in PBS for 1 h. The fixed and permeabilized samples were stained with anti-human type I antibodies (ab34710, Abcam, Cambridge, MA, USA) overnight. Samples were then stained with Alexa Fluor 555-anti-rabbit IgG, Alexa 488-Phalloidin (Life Technology, Carlsbad, CA, USA) and Hoechst dye 33,258 (Thermo Fisher Scientific, Waltham, MA, USA) for 60 min. After staining, a coverslip was mounted onto each sample in the presence of ProLong Gold Antifade Mountant (Thermo Fisher Scientific, Waltham, MA, USA).

To visualize the viable cells on different AMs, HCECs were cultured on different AMs as described in "Assessment of Cell Adhesion to Amniotic Membranes" for 1 or 4 days. At each time point, the medium was removed from each well, and 0.2 ml/well of fresh complete growth medium containing 50 nM Calcein AM (Thermo Fisher Scientific, Waltham, MA, USA) was added to each well. After incubation for 30 min at 37°C, the medium was removed. Cells were washed twice with PBS and ready to be imaged.

To visualize the cell morphology, HCECs cultured on different AMs for 4 days were fixed with 4% paraformaldehyde for 1 h and permeabilized in 0.5% Triton X100 in PBS for 1 h. The fixed and permeabilized cells were stained with Alexa 488-Phalloidin (Life Technology, Carlsbad, CA, USA) for 30 min and observed under an epi-fluorescent microscope (Zeiss Observer D1, Jena, Germany).

2.5 | H&E staining of AMs

Cryosections of AMs were baked at 60°C overnight, fixed in 4% paraformaldehyde for 30 min, and rinsed three times with PBS. Samples were stained in Harris Hematoxylin Solution (Sigma-Aldrich, Inc., St. Louis, MO) for 10 min and rinsed in running tap water for 1 min. Slides were then immersed two times in differentiation solution (0.25 ml concentrated Hydrochloric Acid to 100 ml of 70% alcohol). Subsequently, slides were rinsed under running tap water for 1 min, followed by immersion in Scott's Tap Water Substitute (1% Magnesium

sulfate [MgSO₄] and 0.06% Sodium Bicarbonate) for 60 s. After a 30 s wash in 95% reagent alcohol, samples were counterstained in Alcoholic Eosin Y Solution (Sigma-Aldrich, Inc., St. Louis, MO 68178) for 10 min. After staining was completed, slides were dehydrated by three washes in 100% absolute ethanol, followed by three HistoClear II washes. Slides were mounted using Permount mounting medium (Fisher Scientific Inc.) and imaged using Zeiss Axio Observer A1 microscope.

2.6 | Assessment of cell viability on AMs over time

HCECs (1×10^4 /well) were added to each well of 48-well plates containing pre-conditioned AMs. Three sets of plates were set up and incubated at 37°C with 5% CO₂ and 95% humidity for 1, 4, and 7 days. At the first time point, the medium from each well of all plates was removed, and fresh medium was added. The viability of cells in the first set of plates was measured using the alamarBlue assay. The second and third sets of plates were cultured at 37°C. At the second time point, the viability of cells in the second set of plates was measured. The third set of plates was cultured in fresh medium at 37°C. The viability of cells in the third set of plates was measured using the alamarBlue assay at the third time point.

2.7 | Conditioned media for migration assay

In the test condition, HCECs (2×10^4 /well) were added to each well of 48-well plates containing pre-conditioned AMs. In the control condition, no HCECs were added to the pre-conditioned AMs. After culturing for 24 h, the medium was removed. 0.4 ml/well of fresh growth medium was added to each well with or without cells and incubated at 37°C for 24 h. The supernatants (24-h conditioned media [CM]) were collected from each well and immediately used for the migration assay. The stromal sides of AMs were used for this experiment.

2.8 | Scratch wound migration assay

A 5×10^4 /well HCECs were added to each well of 48-well TCPs and cultured at 37°C with 5% CO₂ and 95% humidity for 2 days. Scratch wounds were made on a confluent monolayer using the tip of a sterile metal rod. The medium was removed, and conditioned medium collected from cells cultured on AMs was added to the wound. Images of the wound areas were captured at 0 h. At minimum, four areas were monitored for each testing group. The plates were incubated at 37°C for 24 h. The exact same wound areas (with marker reference) were imaged at 24 h. Wound areas were measured using ImageJ software (NIH) and expressed in square microns (μm^2). Migrated area = Area_{0h} - Area_{24h}.

2.9 | Stimulation of inflammatory responses of HCECs

A 2×10^4 /well HCECs were seeded and cultured on different AMs for 24 h. Media were removed and fresh medium “-Tumor Necrosis

Factor- α (-TNF- α)” or fresh medium containing 10 ng/ml of human TNF- α (Cat#300-01A, PeproTech Cranbury, NJ) “+TNF- α ” were added to cells and incubated for 24, 48, or 72 h. At each time point, the supernatants were collected for multiplex analysis, and the cells were lysed in 0.2 ml of RNA lysis buffer (Promega, Durham, NC) for quantitative polymerase chain reaction (qPCR) analysis, as described below.

2.10 | Assessment of relative mRNA expressions by qPCR

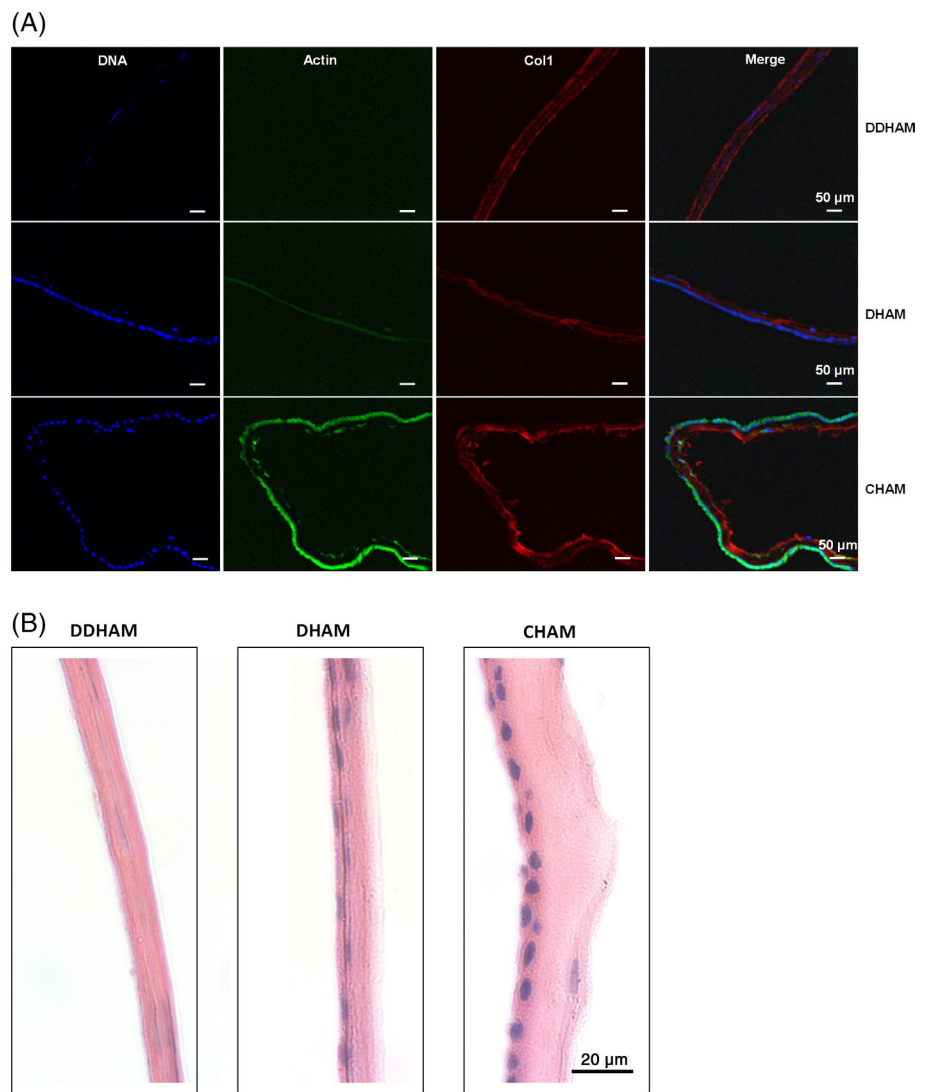
The quantification of the relative gene expression of cytokines by qPCR was performed as previously described.³⁸ Briefly, total RNA from cell lysates was purified using SV 96 Total RNA Isolation System (Promega, Madison, WI, USA). RNA concentration and purity were measured using TECAN Spark Nano plate (TECAN, Morrisville, NC, USA). cDNA preparation and qPCR were performed as previously described.³⁹ The primers for qPCR used for this study were from QuantiTect (Qiagen, Germantown, MD, USA): colony stimulating factor 2 (CSF2: QT00000896), interleukin 6 (IL6: QT00083720), interleukin 8 (IL8: QT00000322), Tumor Necrosis Factor (TNF: QT01079561), and glyceraldehyde 3-phosphate dehydrogenase (GAPDH: QT01192646). Each sample was run in duplicate. After the run was completed, a second derivative analysis was performed using the raw data to determine the mean Cp (Crossing point-PCR-cycle) for each sample. For each gene expression, expression of GAPDH served as an internal control. Relative mRNA expressions were determined by Pfaffl analysis (E ΔCp target/E ΔCp reference) in which primer efficiency $E = 10^{(-1/\text{slope})}$ and $\Delta\text{Cp} = \text{mean Cp of sample} - \text{mean Cp of Control}$. The expression of cells on TCP or the expression of cells at 24 h was used as the “Control” for analyses, which was defined in the specific analysis in “Results.”

2.11 | Statistical methods

In the evaluation of HCEC activity, the independent variables were AM (DDHAM, DHAM, CHAM), side (epithelial, stromal), and time (day 1, day 4, and day 7). The dependent variables were cell adhesion, cell viability, and migration. In the evaluation of HCEC inflammatory response by mRNA expressions, the independent variables were AM (DDHAM, DHAM, CHAM, Control [TCP]), condition (resting, stimulated), and time (24, 48, and 72 h). In the evaluation of HCEC inflammatory response by protein levels, the independent variables were AM (DDHAM, DHAM, CHAM, Control [TCP]) and condition (resting, stimulated, AM only). The dependent variables were relative mRNA expressions of CSF2, IL6, IL8 and TNF, encoding for granulocyte macrophage colony-stimulating factor (GM-CSF), IL-6, IL-8, and TNF- α , respectively.

All analyses were conducted using IBM SPSS (Build 1.0.0.1444). The significance level for all statistical tests was set at $p = .05$. The data were tested and found to be normally distributed. Cell adhesion and migration were analyzed with a two-way analysis of variance (ANOVA) with Tukey post-hoc tests. Cell viability was analyzed with a

FIGURE 1 Staining confirms the absence of cells and nuclei in DDHAM. Immunofluorescent staining of DDHAM, DHAM, and CHAM is shown (A). The cross-sections of the membranes were stained with Hoechst Dye (DNA in blue), phalloidin (Actin in green) and anti-human type I collagen antibodies (Col1 in red). Representative images are shown and the scale bar = 50 μm . H&E staining (nuclei in blue and cytoplasm in red) of DDHAM, DHAM, and CHAM is shown (B). Representative images are shown and the scale bar = 20 μm . Abbreviations: CHAM, cryopreserved human amniotic membrane; DDHAM, decellularized dehydrated human amniotic membrane; DHAM, dehydrated human amniotic membrane



three-way ANOVA with Tukey post-hoc tests. Relative mRNA expressions at 24 h were analyzed with a two-way ANOVA with Tukey post-hoc tests to evaluate each dependent variable in each of the testing conditions. Relative mRNA expressions across time were analyzed with a one-way ANOVA with Tukey post-hoc tests to evaluate each dependent variable in each of the testing conditions. Significant interactions were evaluated with simple main effects analysis with Sidak correction for multiple comparisons. Data are reported as mean \pm standard deviation (SD) within the text and figures. Bars within figures indicate pairwise comparisons.

3 | RESULTS

3.1 | Structure of AMs

To evaluate the structures of these three AMs, cross-sections of AMs were stained for cellular components (DNA and actin) and ECM (type I collagen) (Figure 1A). While strong nuclei staining and actin staining

were detected in DHAM and CHAM, neither actin nor nuclei staining was detected in DDHAM. The presence of type I collagen was detected in all 3 AMs. H&E staining of the three AMs (Figure 1B) confirmed complete decellularization and absence of nuclei in DDHAM. DHAM showed meager staining of dark blue nuclear remnants, while CHAM showed intact dark blue staining for nuclei, showing the presence of cells.

3.2 | Adhesion of HCECs on different AMs

Cell adhesion on different AMs and different sides of AMs was evaluated by comparing cell viability (reflecting the quantity of adhered cells) at 24 h ($n = 4$, Supplementary Table 1). The fluorescence intensity was expressed in arbitrary units (AU).

Effect of sidedness. Cell adhesion was greater on the stromal side than on the epithelial side of AMs (side main effect, $p = .018$), which can be explained by the lower cell adhesion on the epithelial side of DHAM, compared with the stromal side of DHAM ($p < .001$;

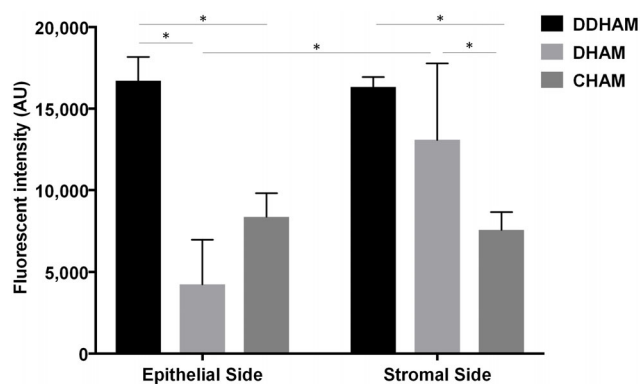


FIGURE 2 The epithelial and stromal sides of DDHAM best support cell adhesion. Human corneal epithelial cells were seeded onto the epithelial and stromal sides of amniotic membranes and incubated for 24 h. A two-way analysis of variance with Tukey post-hoc tests was conducted to evaluate the effects of sidedness and amniotic membrane on cell adhesion. Significant interactions were evaluated with simple main effects analysis with Sidak correction for multiple comparisons. Comparisons between the epithelial and stromal sides of each amniotic membrane are shown, and comparisons between amniotic membranes for each side are shown. Fluorescent intensity is expressed in arbitrary units (AU). Data shown are mean \pm SD ($n = 4$). * $p \leq .05$. Abbreviations: CHAM, cryopreserved human amniotic membrane; DDHAM, decellularized dehydrated human amniotic membrane; DHAM, dehydrated human amniotic membrane

side \times AM, $p = .001$; Figure 2). There was no significant difference between the epithelial and stromal sides of DDHAM ($p = .822$) or between the epithelial and stromal sides of CHAM ($p = .645$).

Effect of AM. Additionally, there was a significant difference in cell adhesion between AMs (AM main effect, $p < .001$), with significantly greater cell adhesion on DDHAM than on DHAM ($p < .001$) and CHAM ($p < .001$). However, as previously indicated, cell adhesion varied with side and AM ($p = .001$; Figure 2). On the epithelial side, cell adhesion was significantly greater on DDHAM than on DHAM ($p < .001$) and CHAM ($p < .001$), and there was no significant difference between CHAM and DHAM ($p = .076$). On the stromal side, cell adhesion was significantly lower on CHAM than on DDHAM ($p < .001$) and DHAM ($p = .014$), and there was no significant difference between DDHAM and DHAM ($p = .207$). These results indicate that among these three AMs, the epithelial and stromal sides of DDHAM best supported cell adhesion.

3.3 | Viability and morphology of HCECs on different AMs on day 4

Live Staining of Epithelial Cells. The viability of HCECs on the stromal side of different AMs (DDHAM, CHAM, DHAM) was observed 4 days after cell seeding (Figure 3A). Consistent with the quantitative results, the HCECs on DDHAM and DHAM appeared to have adhered and spread on day 4 after cell seeding, whereas HCECs on CHAM appeared to be disorganized and adopted a heterogeneous

morphology. The morphology of HCECs on the AMs was monitored by actin staining on day 4 (Figure 3B). The HCECs on DDHAM adapted a cobblestone morphology with a dense actin ring structure.

3.4 | Cell viability on different AMs over time

The viability of cells on different AMs was monitored up to 7 days ($n = 4$, Supplementary Tables 2 and 3). Although the number of viable cells significantly declined over the 7-day culture (time main effect, $p < .001$), cell viability significantly varied with side, AM, and time (side \times AM \times time interaction, $p = .011$). Most notably, cell viability declined for all variables across time, except for the stromal side of DDHAM on day 4 (Figure 4A).

Effect of sidedness. Cell viability was also significantly greater on the stromal side than on the epithelial side of AMs (main effect side, $p < .001$), which can be explained by differences in relative cell viability between sides on days 4 and 7 (Figure 4B). On day 4, the relative cell viability was significantly greater on the stromal side of DDHAM than the epithelial side of DDHAM ($p < .001$), and the relative cell viability was significantly greater on the stromal side of DHAM than the epithelial side of DHAM ($p < .001$). Conversely, the relative cell viability was significantly greater on the epithelial side of CHAM than the stromal side of CHAM ($p = .039$). On day 7, there were no significant differences in relative cell viability between the epithelial and stromal sides of DDHAM ($p = .102$) or CHAM ($p = .157$). However, the relative cell viability was significantly greater on the stromal side of DHAM than the epithelial side of DHAM ($p < .001$).

Effect of AM. Cell number was also significantly different between AMs (main effect AM, $p < .001$) with significantly more viable cells on DDHAM than on DHAM ($p < .001$) and CHAM ($p < .001$) and significantly more viable cells on DHAM than CHAM ($p = .036$). The main effect of AM is largely explained by the significant differences in relative cell viability on days 4 and 7 (Figure 4B).

On the epithelial side on day 4, the relative cell viability was significantly greater on DDHAM than on DHAM ($p = .032$), meanwhile the relative cell viability was similar between DDHAM and CHAM ($p = .978$) and between CHAM and DHAM ($p = .077$). On the epithelial side on day 7, there were no significant differences between the three AMs ($p \geq .219$).

On the stromal side on day 4, the relative cell viability was significantly greater on DDHAM than on CHAM ($p < .001$), and the relative cell viability was significantly greater on DHAM than on CHAM ($p < .001$). There was no significant difference in the relative cell viability on the stromal side on day 4 between DDHAM and DHAM ($p = .477$). On the stromal side on day 7, however, the relative cell viability was significantly lower on CHAM than DDHAM ($p = .003$) and DHAM ($p = .002$). As with the epithelial side, on the stromal side on day 7, there was no significant difference in the relative cell viability between DDHAM and DHAM ($p = .999$).

The findings of higher cell viability on the stromal side of AMs and better maintenance of viability on DDHAM compared with

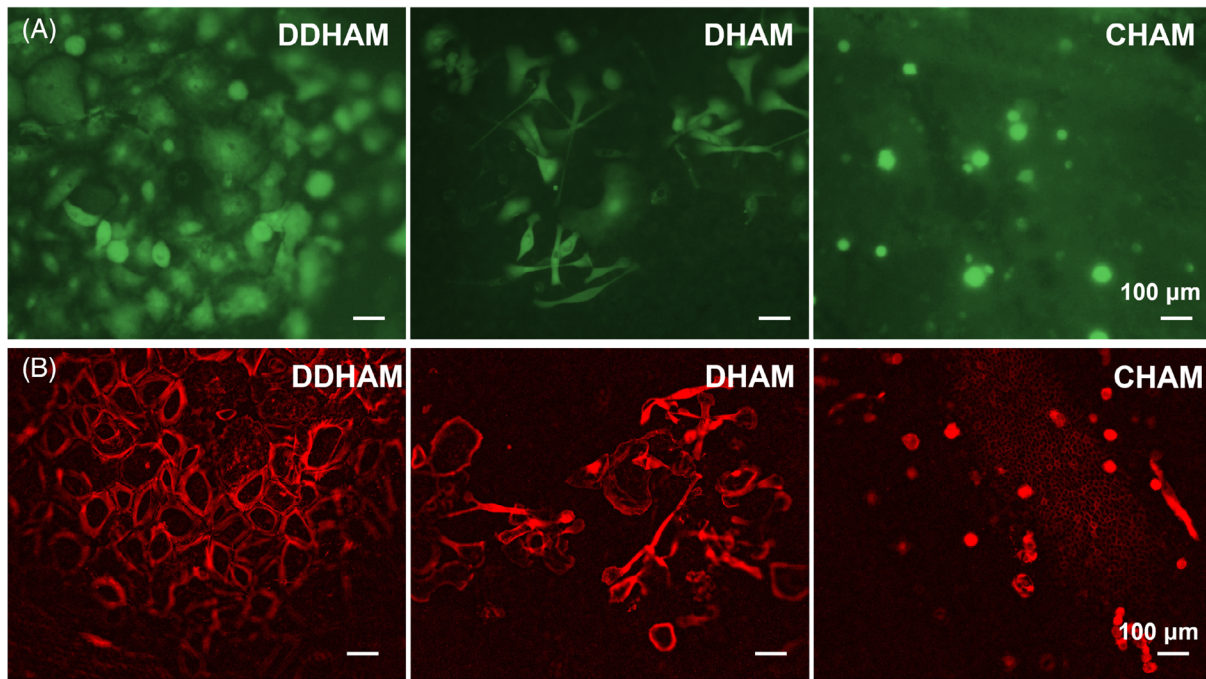


FIGURE 3 Staining confirms human corneal epithelial cell viability and morphology on the stromal side of DDHAM and DHAM on day 4. Human corneal epithelial cells were seeded onto the stromal side of the three amniotic membranes, cultured, and stained with Calcein AM to visualize live cells at day 4 (A). The morphology of human corneal epithelial cells on amniotic membranes was monitored by Actin staining on day 4 and pseudo-colored red (B). Images were captured using epi-fluorescent microscope. Scale bar = 100 μm . Abbreviations: CHAM, cryopreserved human amniotic membrane; DDHAM, decellularized dehydrated human amniotic membrane; DHAM, dehydrated human amniotic membrane

DHAM and CHAM suggests that cell viability was best maintained on the stromal side of DDHAM.

3.5 | Migration of HCECs on different AMs

The CM from different AMs in the absence of HCECs were tested to evaluate the effect of AM alone on the migration of HCECs ($n = 4$, Supplementary Table 4). Additionally, differences in migration were compared between AMs by testing the CM collected from cells cultured on AMs to determine if the factors released by HCECs cultured on different AMs affect cell migration (Supplementary Table 5). Cells cultured on AMs were conditioned for 24 h. The migration of HCECs in the presence of CM from different AMs was evaluated using a scratch wound assay. Wound closure was monitored for 24 h (Figure 5).

There was a significant interaction between the effects of AM and the presence of cells ($p = .006$; Figure 5). Migration was significantly higher with cells than without cells on DDHAM ($p = .009$) and DHAM ($p < .001$). Migration was not significantly different with or without cells on CHAM ($p = .291$) or on the control ($p = .265$).

Effect of AM. Furthermore, among the CM collected in the presence of cells, migration was significantly lower in CM from cells on CHAM than on DDHAM ($p = .004$) and DHAM ($p = .002$). There was no significant difference in migration between DDHAM and DHAM ($p = 1.000$). Compared with the control in the presence of cells,

migration was significantly higher in CM from cells on DDHAM ($p < .001$), DHAM ($p < .001$), and CHAM ($p = .005$).

3.6 | Gene expression of inflammatory cytokines in HCECs

Since the stromal side of AM has been reported to regulate the inflammatory response,^{23,24} the effect of the stromal side of the three AMs on the inflammatory responses of HCECs was evaluated. Cytokines with previously demonstrated roles in wound healing were selected, including GM-CSF, IL-6, IL-8, and TNF- α .⁴⁰⁻⁴⁸ To this end, the inflammatory response of HCECs under an *in vitro* inflammatory condition was mimicked by stimulation with TNF- α for 24 h. The gene expression (relative mRNA levels) of CSF2, IL6, IL8, or TNF in HCECs on different AMs was assessed by qPCR compared with the gene expression in cells cultured on standard cell culture surface, TCP ($n = 3$, Supplementary Table 6).

CSF2. The expression of CSF2 at 24 h varied significantly by stimulation condition (\pm TNF α) and AM ($p = .049$) (Figure 6A). With stimulation, the expression of CSF2 significantly increased on DHAM ($p < .001$), but not DDHAM ($p = .226$), CHAM ($p = .664$), or TCP ($p = .827$). Comparing the expression of CSF2 between AMs in the resting condition showed a similar expression of CSF2 on DDHAM, DHAM, CHAM, and TCP ($p \geq .134$). Comparing the expression of CSF2 between AMs in the stimulated condition showed significantly

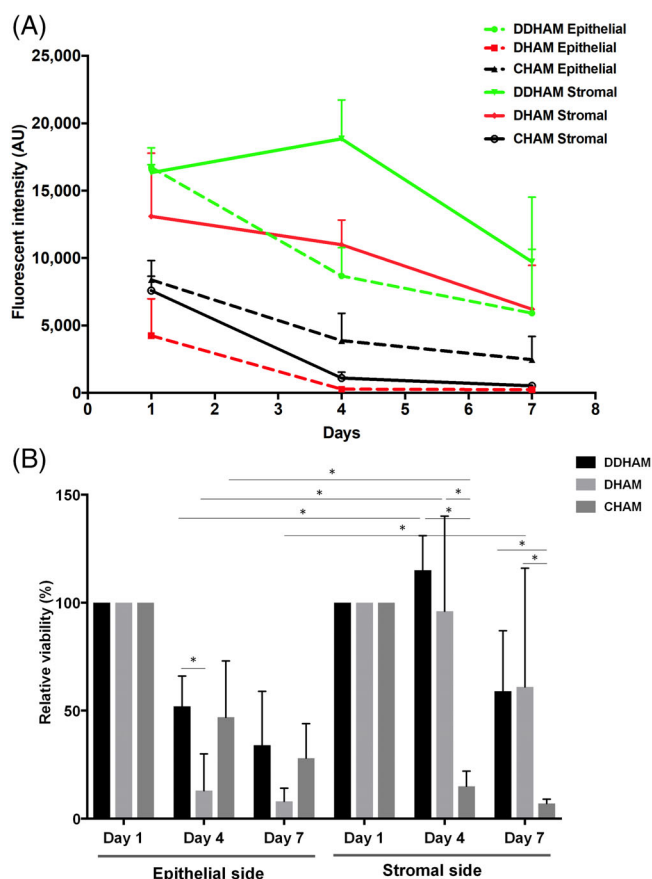


FIGURE 4 Stromal side of DDHAM best supports human corneal epithelial cell viability over time. Human corneal epithelial cells were seeded onto the epithelial and stromal sides of amniotic membranes and incubated for 1, 4 and 7 days. Absolute cell viability is plotted over time for each side of the amniotic membranes (A). The relative cell viability, expressed as a percentage of day 1, is plotted over time for each side of the amniotic membranes (B). A three-way analysis of variance with Tukey post hoc tests was conducted to examine the effects of sidedness, amniotic membrane, and time on relative cell viability. Significant interactions were evaluated with simple main effects analysis with Sidak correction for multiple comparisons. Comparisons between the epithelial and stromal sides of each amniotic membrane are shown and comparisons between the amniotic membranes for each side are shown. Data shown are mean \pm SD ($n = 4$). * $p \leq .05$. Abbreviations: CHAM, cryopreserved human amniotic membrane; DDHAM, decellularized dehydrated human amniotic membrane; DHAM, dehydrated human amniotic membrane

greater expression on DHAM than on DDHAM ($p = .001$), CHAM ($p < .001$), and TCP ($p < .001$).

IL6. The expression of *IL6* at 24 h varied significantly by stimulation condition and AM ($p = .002$) (Figure 6B). With stimulation, the expression of *IL6* significantly increased on DDHAM ($p < .001$), CHAM ($p = .017$), and TCP ($p = .014$), but not DHAM ($p = .128$). Comparing the expression of *IL6* between AMs in the resting condition showed a similar expression of *IL6* on DDHAM, DHAM, CHAM, and TCP ($p \geq .717$). In the stimulated condition, there was significantly higher expression of *IL6* on DDHAM than on DHAM ($p < .001$), CHAM ($p < .001$), and TCP ($p < .001$).

IL8. Although the expression of *IL8* at 24 h did not vary significantly by stimulation condition and AM ($p = .188$), there were main effects for stimulation condition ($p < .001$) and AM ($p = .002$) (Figure 6C). The overall expression of *IL8* significantly increased with stimulation. Post-hoc analyses revealed that overall *IL8* expression was significantly greater on DHAM than CHAM ($p = .018$) and TCP ($p = .014$) and on DDHAM than CHAM ($p = .022$) and TCP ($p = .017$). There was no significant difference in *IL8* expression between DHAM and DDHAM ($p = 1.000$) or between CHAM and TCP ($p = .999$).

TNF. Although the expression of *TNF* at 24 h did not vary significantly by stimulation condition and AM ($p = .194$), there were main effects for stimulation condition ($p = .001$) and AM ($p < .001$) (Figure 6D). The overall expression of *TNF* significantly increased with stimulation. Post-hoc analyses revealed that overall *TNF* expression was significantly greater on DDHAM than CHAM ($p < .001$) and TCP ($p < .001$) and on DHAM than CHAM ($p = .022$) and TCP ($p = .024$). There was no significant difference in *TNF* expression between DDHAM and DHAM ($p = .095$) or between CHAM and TCP ($p = 1.000$).

These results indicate that at 24 h, the presence of DDHAM and DHAM stimulated the expression of *CSF2*, *IL6*, *IL8*, and *TNF* in HCECs more than cells on CHAM or TCP.

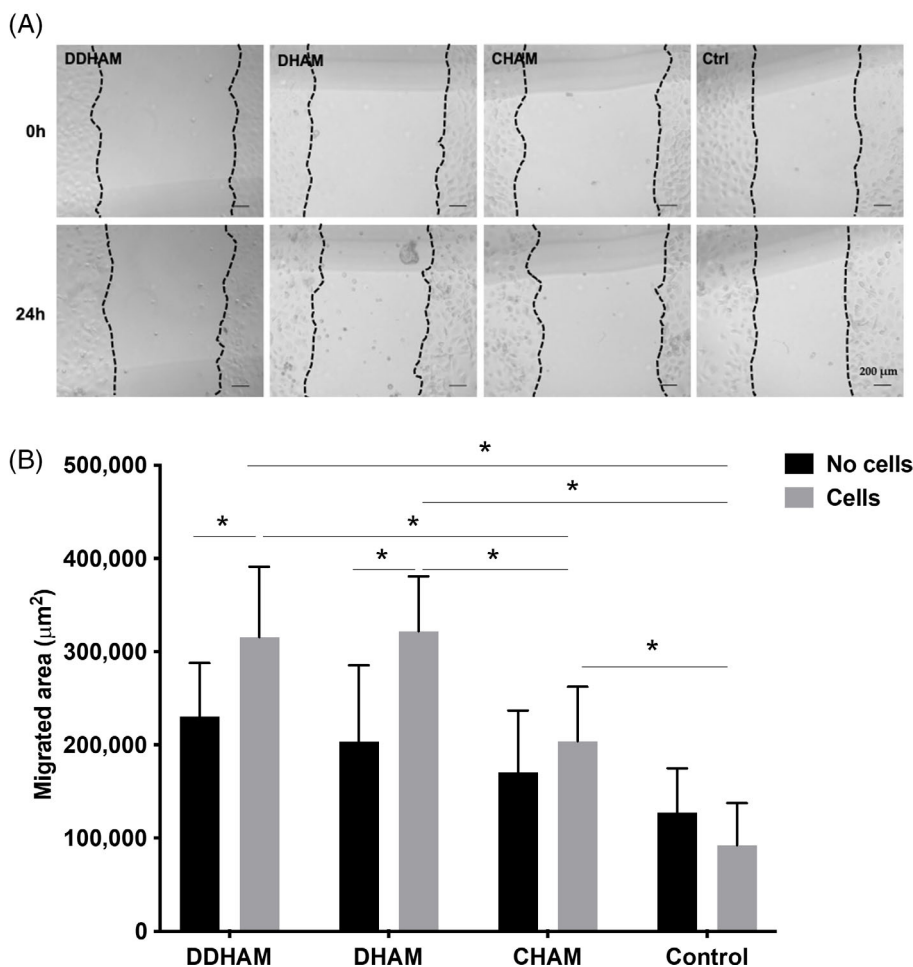
3.7 | Gene expression of inflammatory cytokines in HCECs over time

The inflammatory response is a dynamic process. The expression of cytokines at different time points indicates the stage in the wound healing process. To evaluate the expression of cytokines over a 72-h time course, the expression of each cytokine was analyzed at 24-h intervals (Figure 7; $n = 3$, Supplementary Table 7).

There were no significant changes across time in the expression of *CSF2* in the stimulated condition for DDHAM ($p = .206$), DHAM ($p = .078$), or CHAM ($p = .215$) (Figure 7A). TCP was an exception with significant changes across time in the expression of *CSF2* in the stimulated condition ($p < .001$). The expression of *CSF2* on TCP significantly increased from 24 to 72 h ($p < .001$) and from 48 to 72 h ($p < .001$). *CSF2* expression on TCP remained similar from 24 to 48 h ($p = .700$).

IL6. There were statistically significant changes in the expression of *IL6* in the stimulated condition across time on DDHAM ($p = .007$), DHAM ($p < .001$), CHAM ($p < .001$), and TCP ($p = .002$) (Figure 7B). The expression of *IL6* on DDHAM showed significant declines from 24 to 72 h ($p = .007$) and from 48 to 72 h ($p = .021$). *IL6* expression on DDHAM remained similar from 24 to 48 h ($p = .623$). The expression of *IL6* on DHAM showed a significant increase from 24 to 48 h ($p = .003$) and then a significant decrease from 48 to 72 h ($p < .001$). *IL6* expression on DHAM remained similar from 24 to 72 h ($p = .321$). Comparing the expression of *IL6* on CHAM showed significant declines from 24 to 48 h ($p < .001$) and from 24 to 72 h ($p < .001$). *IL6* expression on CHAM was non-detectable at both 48 and 72 h. The expression of *IL6* on TCP showed a significant increase from 24 to

FIGURE 5 Migration is greatest on DDHAM and DHAM in the presence of human corneal epithelial cells. Representative scratch wound images are shown to demonstrate the effects of conditioned media on the migration of human corneal epithelial cells at 0 and 24 h. Scale bar = 200 μm (A). The conditioned media from different amniotic membranes (with and without cells) were tested to evaluate the effect of amniotic membranes alone on the migration of human corneal epithelial cells (B). A two-way analysis of variance with Tukey post-hoc tests was conducted to evaluate the effects of cell presence and amniotic membrane on cell migration. Significant interactions were evaluated with simple main effects analysis with Sidak correction for multiple comparisons. The wound areas (μm^2) were measured using Image J. The migrated area = Area_{0h} – Area_{24h}. Data shown are mean \pm SD ($n = 4$). * $p \leq .05$. Abbreviations: CHAM, cryopreserved human amniotic membrane; DDHAM, decellularized dehydrated human amniotic membrane; DHAM, dehydrated human amniotic membrane; Medium Ctrl, medium control



48 h ($p = .008$) and then a significant decline from 48 to 72 h ($p = .002$). *IL6* expression on TCP remained similar from 24 to 72 h ($p = .407$).

IL8. Although there were statistically significant changes in the expression of *IL8* in the stimulated condition across time on CHAM ($p = .024$) and TCP ($p < .001$), *IL8* expression remained similar across time on DDHAM ($p = .179$) and DHAM ($p = .282$) (Figure 7C). The expression of *IL8* on CHAM significantly increased from 24 to 72 h ($p = .040$) and from 48 to 72 h ($p = .033$). *IL8* expression on CHAM remained similar from 24 to 48 h ($p = .984$). Like CHAM, the expression of *IL8* on TCP significantly increased from 24 to 72 h ($p < .001$) and from 48 to 72 h ($p < .001$). *IL8* expression on TCP remained similar from 24 to 48 h ($p = .071$).

TNF. Although there were statistically significant changes in the expression of *TNF* in the stimulated condition across time on DHAM ($p < .001$) and TCP ($p = .005$), *TNF* expression remained similar across time on DDHAM ($p = .125$) and CHAM ($p = .519$) (Figure 7D). The expression of *TNF* on DHAM significantly increased from 24 to 48 h ($p = .009$) and significantly declined from 24 to 72 h ($p = .048$), and from 48 to 72 h ($p < .001$). In addition, the expression of *TNF* on TCP showed significant increases from 24 to 48 h ($p = .035$) and from 24 to 72 h ($p = .004$). *TNF* expression on TCP remained similar from 48 to 72 h ($p = .201$).

The changes in relative mRNA levels across time showed different trends for different AMs and cytokines. While the expression levels increased over time in cells cultured on TCP, the expression of such cytokines showed a trend of decline in cells cultured on DDHAM.

4 | CLINICAL CASE STUDY

An 87-year-old female presented with a chief complaint of left eye deterioration, occurring over the previous few months. She reported difficulty seeing small print, due to discomfort and a foreign body sensation with prolonged reading. Her medical history was significant for dry eye syndrome, primary open-angle glaucoma, epiretinal membrane, and macular drusen in both eyes. Supportive treatments included lubricant eye drops, hyperosmotic agents, and bandage contact lenses. Her ophthalmic surgical history consisted of cataract extraction in both eyes and YAG laser capsulotomy in both eyes. Upon examination, epithelial and sub-epithelial scarring in map/dot configuration was noted. Based on her presentation, history, and careful examination of the cornea, the patient was diagnosed with anterior basement membrane dystrophy (ABMD). With the patient's consent, the decision was made to treat the anterior basement membrane

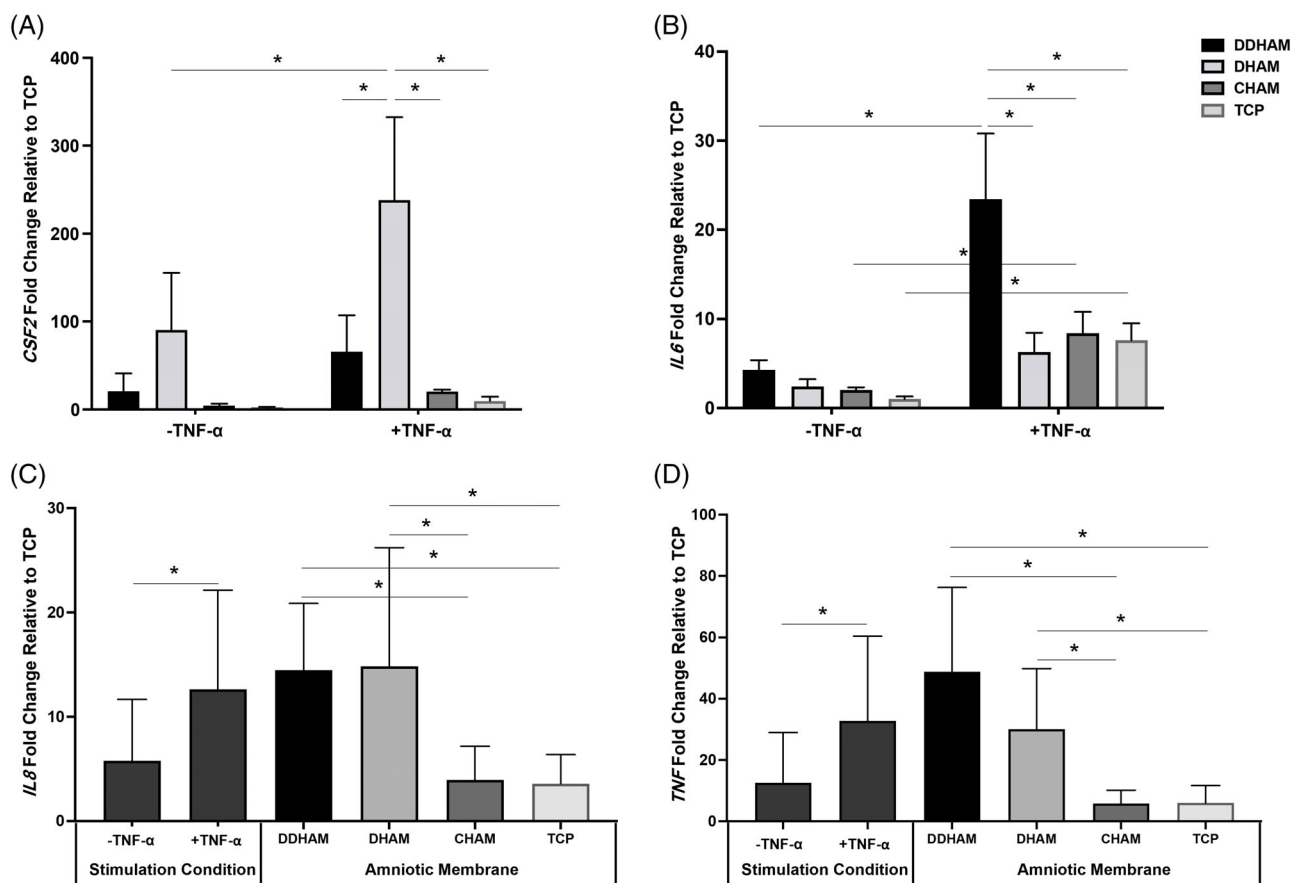


FIGURE 6 DDHAM and DHAM support an inflammatory response at 24 h. Relative mRNA expressions of *CSF2* (A), *IL6* (B), *IL8* (C), and *TNF* (D) at 24 h are shown. Relative mRNA expressions at 24 h are normalized to TCP in the resting condition. A two-way analysis of variance with Tukey post-hoc tests was conducted to evaluate the effects of stimulation condition and amniotic membrane on mRNA expressions at 24 h. Significant interactions were evaluated with simple main effects analysis with Sidak correction for multiple comparisons. Data shown are mean \pm SD ($n = 3$). * $p \leq .05$. Abbreviations: CHAM, cryopreserved human amniotic membrane; *CSF2*, colony-stimulating factor 2; DDHAM, decellularized dehydrated human amniotic membrane; DHAM, dehydrated human amniotic membrane; *IL6*, interleukin 6; *IL8*, interleukin 8; TCP, tissue culture plate; *TNF*, tumor necrosis factor

dystrophy surgically, using DDHAM as a substrate to repopulate the anterior corneal surface with normal Bowman's membrane (i.e., epithelium and epithelial basement membrane).

Debridement of the corneal epithelium and Bowman's membrane was performed, and an AM was placed (without sutures) as an outpatient procedure. A local anesthetic was applied, and the irregular surface epithelium was visualized (Figure 8A). A diamond burr was used to remove all abnormal, loose corneal epithelium (Figure 8B) as well as the underlying sub-epithelial scarring and ABMD debris gently and uniformly (Figure 8C). The epithelial surface was then rinsed with balanced salt solution. The DDHAM was carefully placed over the debrided membrane (Figure 8D) and covered with a bandage contact lens to help with discomfort and healing (Figure 8E).

Postoperatively, the patient was instructed to use a steroid/antibiotic drop four times per day for 10 days, which was slowly tapered over six weeks. She was seen postoperatively at one day, three days, one week, two weeks, one month, and two months. On postoperative day one, the patient reported discomfort due to the large abrasion from the surgery. On postoperative day three, however, the patient

reported that the discomfort had subsided. Almost immediately, the patient reported improved comfort in activities of daily living. At the 1-month postoperative visit, the graft had fully dissolved into the tissue and no remnants were visible. The corneal surface was smooth and recognizable as normal (Figure 8F). Given the patient's history of treatment with bandage contact lenses and continued discomfort, the noted improvements are presumably attributable to the presence of the DDHAM.

5 | DISCUSSION

The structure of the AM basement membrane is hypothesized to promote epithelialization on the ocular surface. The collagen composition closely resembles that of the conjunctiva and cornea, making the AM a suitable substrate for the growth of epithelial cells. The AM promotes the growth of corneal epithelium through four proposed mechanisms:^{3,5} (1) the facilitation of epithelial cell migration^{7,6,49} (2) the reinforcement of basal epithelial cell adhesion,⁴⁹⁻⁵¹ (3) the promotion

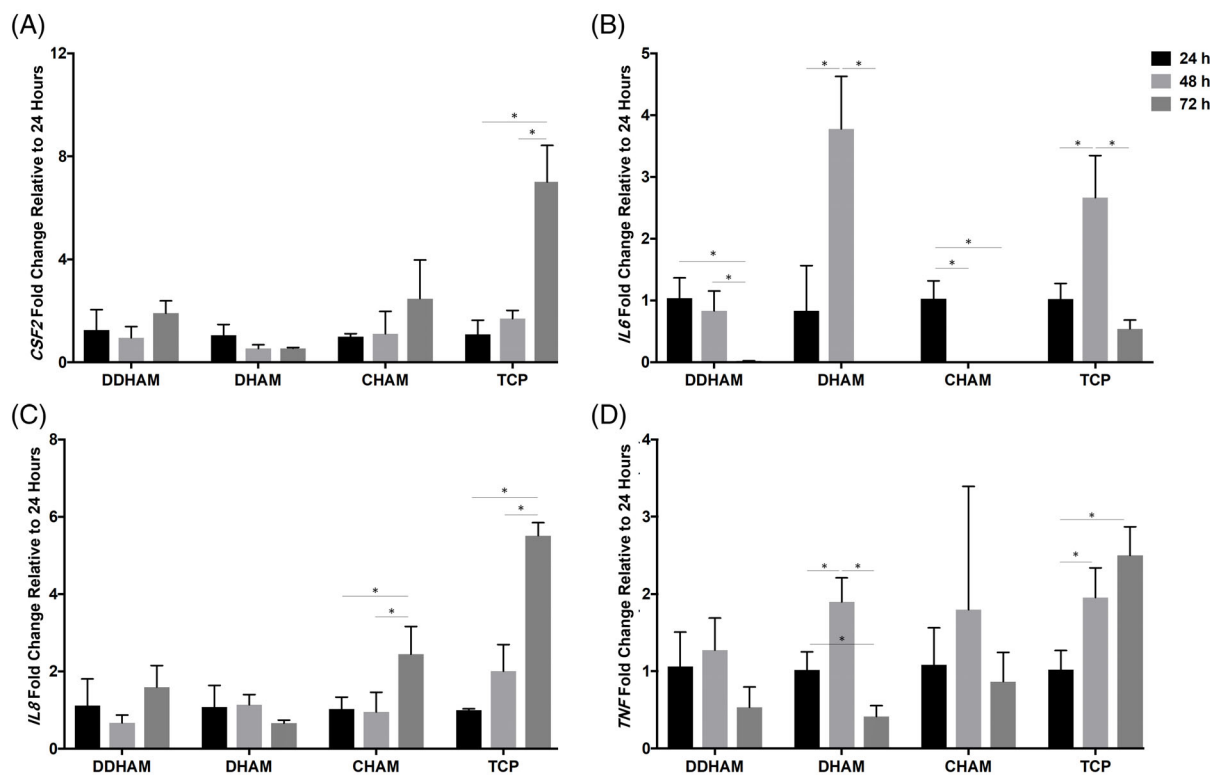


FIGURE 7 DDHAM supports a declining inflammatory response across time. Relative mRNA expressions of *CSF2* (A), *IL6* (B), *IL8* (C), and *TNF* (D) across time in the stimulated condition (+TNF- α) are shown. Relative mRNA expressions across time are normalized to expression at 24 h. A one-way analysis of variance with Tukey post-hoc tests was conducted to examine the effect of time on mRNA expressions. Statistical comparisons are between time points for each amniotic membrane in the stimulated condition (+TNF- α). Data shown are mean \pm SD ($n = 3$). * $p \leq .05$. Abbreviations: CHAM, cryopreserved human amniotic membrane; *CSF2*, colony-stimulating factor 2; DDHAM, decellularized dehydrated human amniotic membrane; DHAM, dehydrated human amniotic membrane; *IL6*, interleukin 6; *IL8*, interleukin 8; TCP, tissue culture plate; *TNF*, tumor necrosis factor

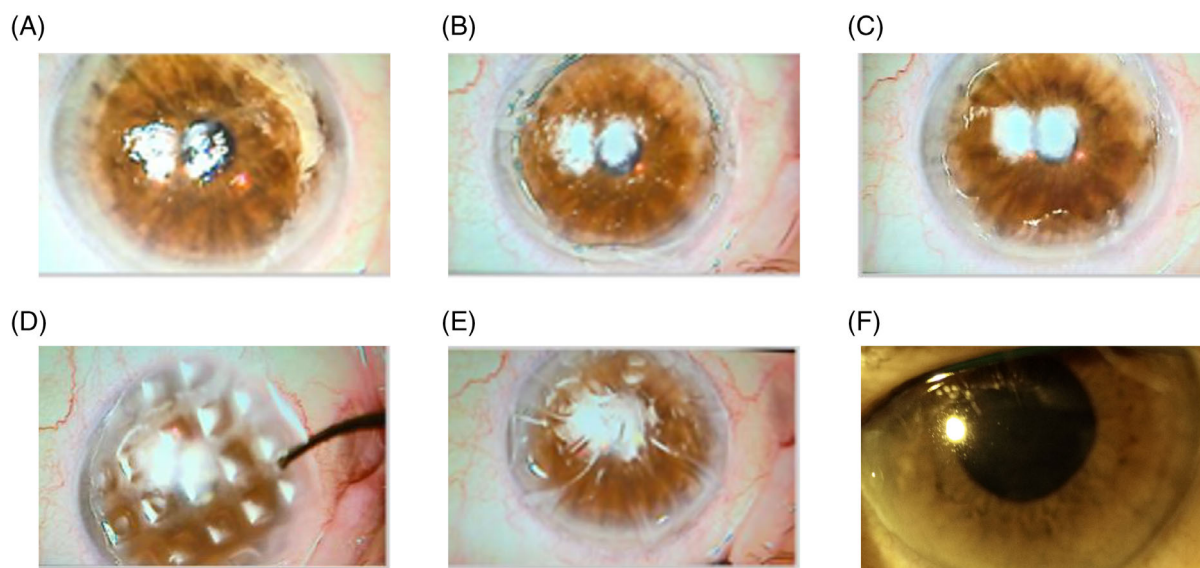


FIGURE 8 Successful clinical application of DDHAM to treat a case of anterior basement membrane dystrophy. Images of the epithelial surface were taken to illustrate the clinical course: pre-operatively, showing the poor irregular surface of the epithelium (A), post removal of poor epithelium with visible sub epithelial debris from Anterior Basement Membrane Dystrophy (B), post burring of all sub-epithelial scarring and Anterior Basement Membrane Dystrophy debris (C), placement of DDHAM (D), placement of bandage contact lens over DDHAM (E), and two months postoperatively, showing a clear surface (F)

of epithelial cell differentiation,^{52–54} and (4) the prevention of apoptosis.^{55,56} Although there is evidence that the stromal surface can support epithelial cell growth,²⁶ epithelialization is believed to occur preferentially on the basement membrane.²⁵ However, most of the existing research is limited to cryopreserved AMs, making it unclear whether these findings are applicable to differently processed AMs.

Different processing methodologies have the potential to alter the cellular content and structure of the AM with the potential to impact the functional characteristics of ECM.³⁰ Previous work has demonstrated significant differences in composition and ultrastructure between DDHAM and CHAM.²⁸ Although cryopreservation is one of the most widely used preservation techniques, it has some disadvantages, namely, impacting the viability and proliferative capacity of cells as well as the need to be shipped and stored at -80°C .⁵⁷ Therefore, the present study sought to compare how sidedness and different methods of sterilization, preservation, and decellularization impact HCEC adhesion, viability, and migration. As indicated in previous reports,³⁵ the authors postulate that an ideal ocular AM requires the removal of cells, DNA, cellular debris, and residual growth factors and cytokines as well as adequate preservation of the native ECM architecture and bioactive components to prevent an inflammatory response and promote dynamic interactions between the ECM and host cells. The present study results support our hypothesis. First, the study demonstrated that DDHAM is a fully decellularized AM, whereas DHAM and CHAM contain residual cells and DNA. The study also found that DDHAM best supported the cellular activities of HCECs. In addition, the presence of DDHAM enhanced an initial inflammatory response and prevented a prolonged inflammatory response in HCECs under an *in vitro* inflammatory condition.

5.1 | Staining confirms the absence of cells and nuclei in DDHAM

Previous research documents that the biological effectiveness of AMs in ophthalmology is facilitated by its ECM, rather than cells preserved in the AM.^{23,57,58} In decellularized AM, the ECM is presumed to serve as a physical conduit for cellular infiltration, whereby the host cells and ECM interact to provide the necessary biochemical stimulus to activate a healing response.³⁵ Therefore, as a preliminary step, staining was performed on each of the three AMs to visualize the cellular content and structure. Both immunofluorescent and H&E staining confirmed complete decellularization and the absence of nuclei in DDHAM, whereas both DHAM and CHAM showed nuclear content, remnants in DHAM and the presence of cells in CHAM.

5.2 | Stromal side of DDHAM best supports the cellular activities of HCEC

The results from this *in vitro* investigation suggest that the stromal side of DDHAM best supports HCEC activity. Sidedness did not impact HCEC adhesion on DDHAM or CHAM, but HCEC adhesion

was significantly lower on the epithelial side of DHAM. The difference in cellular adhesion between DDHAM and DHAM, two dehydrated AMs, suggests that the removal of cellular components, DNA, growth factors and cytokines provides a more cell-friendly environment, supporting the attachments of HCECs. Future research should more fully evaluate the mechanical properties of differently processed AMs, as these differences may help explain the disparities in HCEC adherence.⁵⁹

When examined across time, cell viability was found to decrease for all sidedness and AM combinations, except for the stromal side of DDHAM. On the stromal side of DDHAM, cell viability increased from day 1 to day 4. The specific cause of the overall decrease in cell viability is not clear. The presence of amnion cells (cryopreserved or dried) in the CHAM or DHAM may inhibit the ability of these AMs to support corneal cell proliferation. Although it has been reported previously that decellularized AM is a better substrate than fresh amnion for corneal epithelial cells,⁶⁰ these results suggest that sidedness may also be a factor. This study found that the stromal side of DDHAM is the most compatible substrate for the growth of HCECs, whereas neither the epithelial or stromal sides of CHAM and DHAM appear to consistently support their adhesion or growth.

These findings are further supported by staining. On day four, DDHAM demonstrated the most homogeneous growth pattern of HCECs (Figure 3). As indicated by actin staining, the morphology and organization of cells on DDHAM is similar to the morphology of corneal epithelial cells *in situ* (Figure 4).⁶¹ These observations suggest orderly growth on the AM. Conversely, the growth pattern on DHAM appears disorganized, and it remains unclear whether the HCECs on CHAM are viable or existent. It has been well established that when cells are stressed, they change phenotype.⁶² While there are many factors to consider, these results suggest that the differences in the dehydration, cryopreservation, and decellularization processes may impact how the cells interact with the membrane, specifically in terms of cell adhesion and cell viability.

Differently processed AMs may also affect the release of factors from epithelial cells cultured on them. To evaluate the effect of AM alone on the migration of HCECs, the present study tested the CM from three different AMs without cells. This experiment was also performed with CM collected from cells cultured on AMs to understand if the cells release additional factors when cultured on AMs to promote migration to a greater extent than the AM alone. This study found that HCECs migrated more in the presence of CM with cells than without cells on DDHAM and DHAM. However, there was no difference in HCEC migration in the presence of CM with or without cells on CHAM or on the control. These findings suggest that the factors released by the cells promote cell migration beyond that of the AM (i.e., DDHAM and DHAM) alone. In addition, the migration of HCEC in the presence of CM from cells on DDHAM and from cells on DHAM were comparable, and both were significantly greater than cells on CHAM. One possible explanation of this finding is that there were fewer cells on CHAM when the conditioned medium was collected. With fewer cells, the stimulatory effect of the CM may be lower, resulting in less migration in the presence of conditioned

medium from cells on CHAM. Additionally, the migration of HCECs in the presence of CM with cells was significantly greater on all three AMs than the medium control. Collectively, these findings suggest that factors released from cells and AMs promote cell migration and that the factors released vary by AM, resulting in more HCEC migration on DDHAM and DHAM than CHAM. Additional studies are needed to determine the identity and source of these factors.

An additional independent experiment was conducted to determine whether sidedness influences HCEC migration. The experiment followed the same methodology as described in the “Conditioned Media for Migration Assay” and “Scratch Wound Migration Assay” sections. In this experiment, however, the migration of HCECs in the presence of CM was evaluated on both the stromal and epithelial sides of the AMs. The results from this experiment confirmed that there is no difference in HCEC migration in the presence of CM from cells on the epithelial or on stromal sides of the AMs ($p = .407$; data not shown).

Traditionally, the AM is placed as a graft with epithelial side up to promote epithelialization over a defect. Both DHAM and CHAM have this clinical applicability due to their sidedness. However, DDHAM is manufactured with the stromal side facing out to interface with the ocular surface regardless of orientation. The results from this in vitro study demonstrated that HCEC activity was highest on the stromal side of DDHAM, thus supporting its clinical applicability as a graft. Moreover, the included case study demonstrated the successful application of DDHAM to treat ABMD. One-month postoperatively, the corneal surface was smooth and recognizable as normal, which could be indicative of progressing re-epithelialization. However, histology at additional time points is necessary to demonstrate reorganization and remodeling of the corneal epithelium, its basement membrane, and Bowman's layer. It is also important to note that a more normal epithelium can grow back after debridement in the absence of an AM or other biomaterial. Therefore, it remains unclear whether these findings are in fact due to the presence of the DDHAM. While encouraging, additional, in vivo investigations with a larger sample size are needed to evaluate DDHAM more fully as well as its ability to promote epithelialization on the ocular surface.

5.3 | DDHAM supports an initial inflammatory response, followed by a declining trend across time

The anti-inflammatory properties of AM have been well documented.¹⁰⁻¹² Based on in vitro research, AMs reduce the expression of growth factors and pro-inflammatory cytokines from the damaged ocular tissue⁶³ while also trapping inflammatory cells and inducing apoptosis.^{23,24} Therefore, the secondary aim of this investigation was to evaluate the inflammatory response of HCECs on different AMs. This was accomplished by examining the immediate mRNA expressions as well as trends across time. Given their known roles in corneal wound healing, the pro-inflammatory cytokines, GM-CSF, IL-6, IL-8, and TNF- α were selected to assess the inflammatory response of HCECs.

GM-CSF is recognized as both an inflammatory⁶⁴ and immunoregulatory cytokine⁶⁵ with its effects dependent on dose and context.⁶⁵⁻⁶⁷ This multipotent cytokine has been recognized for having important roles in inflammation and wound healing and has a proven ability to enhance corneal wound healing in vitro and in vivo.⁴⁰ Interleukin-6, IL-8, and TNF- α are more traditional pro-inflammatory cytokines. In addition to regulating inflammatory and immune responses, IL-6 has been shown to facilitate corneal wound healing in vitro and in vivo.⁴¹⁻⁴⁴ IL-8 is a corneal factor that induces neovascularization and is thought to modulate wound healing.^{45,46} Lastly, TNF- α is involved in the corneal inflammatory response and wound healing following corneal injuries.^{47,48}

In the present study, there was a higher expression of *IL6*, *IL8*, and *TNF* in cells cultured on DDHAM in the first 24 h, followed by a declining trend across time. These observations suggest that the presence of DDHAM may promote an initial inflammatory response and prevent a prolonged inflammatory response in HCEC cells, which may be advantageous in a wound healing environment. However, additional in vivo research is needed to evaluate these findings more fully.

The AM is used for ocular surface reconstruction to treat a wide variety of ocular pathologies, including corneal surface disorders with and without limbal stem cell deficiency,^{68,69} reconstruction of the conjunctival surface (e.g., pterygium removal),^{70,71} as a carrier for ex vivo expansion of limbal epithelial cells,^{72,73} glaucoma,⁷⁴ neoplasia,⁷⁵ sclera melts and perforations,^{76,77} among others. Given its potential to enhance healing, integrate with host tissue, and avoid a foreign body response, decellularized AM has gained increasing interest in recent years.^{28,30,60,78-82} Adequate preservation of the ECM in decellularized AM has been shown to improve the interaction of various cell types within the AM, with evidence of improved cell adhesion, proliferation, and differentiation.^{60,78-82} Moreover, and perhaps most importantly, decellularized AM has been shown to integrate into biological tissue with low immunogenicity.^{78,80,82}

There is a growing body of evidence, evaluating the use of AMs in strabismus surgery.⁸³⁻⁸⁹ Similar to the present study, a 2019 review article evaluated the use of AMs with different processing methodologies for extraocular muscle surgery.⁸⁹ The authors concluded that dried AM does not effectively limit adhesion formation.⁸⁹ This conclusion, however, is based on the results from three animal studies^{84,85,87} and two case reports.^{88,90} Notably, however, one of the two case reports described a positive outcome.⁸⁸ That being said, the AM was applied to create a barrier between a titanium plate and adjacent muscle and therefore, was not used in the same capacity as the other studies. Given the limited clinical evidence, additional clinical reports are needed to more fully evaluate whether dried AM can effectively prevent adhesion formation in strabismus surgery and in other ocular procedures.

Also relating to the current study, Kassem and colleagues compared the transplantation of AMs in different orientations during extraocular muscle surgery in rabbits.⁸³ The AM was wrapped around the muscle with either the epithelium in contact with the muscle or

the stroma in contact with the muscle. In a third group, the AM was folded on itself with the epithelium facing outward. Notably, the study found no difference in adhesion formation between the three AM groups. This finding suggests that the orientation of the AM does not influence adhesion formation in strabismus surgery. Additional work is needed to determine if AM orientation influences the outcomes in other ocular procedures.

These two previous reports^{83,89} contrast with the results presented here. In our study, the stromal side of DDHAM, a dehydrated AM, was found to best support HCEC function. There are a number of possibilities that may explain these differences. First, the in vitro design has its own inherent set of limitations. Most notably, the inability to replicate the complexities and cellular interactions of an in vivo environment. Second, the present report did not specifically examine adhesion formation, but rather examined the direct interaction between the AMs and HCECs. In our opinion, based on the available evidence, additional comparative studies are needed to determine whether AM processing and orientation influence clinical outcomes.

AmbioDry™ is a single-layer AM that has been low-dose electron beam sterilized and preserved through dehydration with the epithelial layer mechanically eliminated.⁹¹ Although the product is no longer available, much can be garnered from the scientific evaluation of this DDHAM product.^{59,92} Memarzadeh et al. demonstrated its ability to act as an effective conjunctival autograft in preventing pterygium recurrence.⁹² Additionally, a biomechanical research study confirmed that this DDHAM maintains desirable elastic characteristics when rehydrated, making it an easy-to-manipulate tissue for ocular surface reconstruction.⁵⁹ Despite distinct differences between AmbioDry™ and Biovance®3L Ocular, such as Biovance®3L Ocular's unique three-layer design as well as its complete removal of cells and associated growth factors,³⁵ these previous publications provide additional insight into DDHAM products and their clinical application in ophthalmology.

While the results from the present study are encouraging, there are several limitations. First and foremost, findings from in vitro investigations do not directly translate to clinical application. A superb compatibility with ocular epithelial cells does not necessarily equate to clinical improvements in ocular wound healing. In addition, the alamarBlue assay, like other metabolic activity assays, has inherent limitations. The alamarBlue assay is sensitive to changes in cell metabolism as well as cell number. Therefore, fluorescence intensity measured with the alamarBlue assay may not directly reflect the number of adherent cells and should be interpreted carefully. To avoid this limitation, we considered DNA quantification to reflect the number of cells on the AMs. Since two of the AMs included in the study contain the DNA of amniotic cells (i.e., DHAM and CHAM), the extraction and quantification of DNA is increasingly complicated. Therefore, the alamarBlue assay was chosen as our means of measurement. Although the present study did not include an evaluation of the functional characteristics of the cells adhered to the different AMs (e.g., transepithelial/transendothelial electrical resistance [TEER] measurement, ZO-1 staining, or fluorescein permeability), this would provide a more

comprehensive understanding of the permeability of different AMs and is therefore, an important direction for future work. Unlike this in vitro study, many types of cells exist and interact with each other in tissues in vivo. The cellular behavior of one cell type does not necessarily represent the responses of the tissue. Despite these limitations, however, this study is unique in its comparison of ocular cell activity and inflammatory response on three commercially available AMs. Furthermore, this study is the first to demonstrate the effect of AM sidedness on cellular activities.

6 | CONCLUSION

Overall, DDHAM was shown to support better HCEC functionality in vitro, which may suggest greater ocular cell compatibility in vivo. Additional research is warranted to evaluate the wound healing response of DDHAM as well as its clinical application and outcomes.

ACKNOWLEDGMENTS

Nikita John acknowledges support from the Aresty Research Center at Rutgers University. The authors acknowledge Luis Martinez, BS, MBA for his critical role in study design and project management.

FUNDING INFORMATION

This study was partially funded by Celularity Inc. (170 Park Ave., Florham Park, NJ, 07932) and the Laboratory for Biomaterials Research at Rutgers University (145 Bevier Road, Piscataway, NJ 08854).

CONFLICT OF INTEREST

Adam Kuehn, Desiree Long, Raja Sivalenka, Radoslaw A. Junka, Anna Gosiewska, Stephen A. Brigido, and Robert J. Hariri are salaried employees at Celularity Inc. Anish Shah functions as a key opinion leader for Celularity Inc. Yong Mao reports a grant from Celularity Inc. during the study. Nicole M. Protzman serves as an independent contractor for Celularity Inc. and reports personal fees from Celularity Inc. during the study. Nikita John has nothing to disclose.

DATA AVAILABILITY STATEMENT

The data that supports the findings of this study are available in the supplementary material of this article.

ORCID

Anna Gosiewska  <https://orcid.org/0000-0003-0157-7875>

REFERENCES

1. Leal-Marín S, Kern T, Hofmann N, et al. Human amniotic membrane: a review on tissue engineering, application, and storage. *J Biomed Mater Res B Appl Biomater.* 2021;109:1198-1215.
2. Liu J, Li L, Li X. Effectiveness of cryopreserved amniotic membrane transplantation in corneal ulceration: a meta-analysis. *Cornea.* 2019; 38:454-462.
3. Malhotra C, Jain AK. Human amniotic membrane transplantation: different modalities of its use in ophthalmology. *World J Transplant.* 2014;4:111-121.

4. Fernandes M, Sridhar MS, Sangwan VS, Rao GN. Amniotic membrane transplantation for ocular surface reconstruction. *Cornea*. 2005;24:643-653.
5. Walkden A. Amniotic membrane transplantation in ophthalmology: an updated perspective. *Clin Ophthalmol*. 2020;14:2057-2072.
6. Meller D, Pauklin M, Thomasen H, Westekemper H, Steuhl KP. Amniotic membrane transplantation in the human eye. *Dtsch Arztebl Int*. 2011;108:243-248.
7. Meller D, Pires RT, Tseng SC. Ex vivo preservation and expansion of human limbal epithelial stem cells on amniotic membrane cultures. *Br J Ophthalmol*. 2002;86:463-471.
8. Shayan Asl N, Nejat F, Mohammadi P, et al. Amniotic membrane extract eye drop promotes limbal stem cell proliferation and corneal epithelium healing. *Cell J*. 2019;20:459-468.
9. Meller D, Tseng SC. Conjunctival epithelial cell differentiation on amniotic membrane. *Invest Ophthalmol Vis Sci*. 1999;40:878-886.
10. Sharma N, Singh D, Maharana PK, et al. Comparison of amniotic membrane transplantation and umbilical cord serum in acute ocular chemical burns: a randomized controlled trial. *Am J Ophthalmol*. 2016;168:157-163.
11. Tabatabaei SA, Soleimani M, Behrouz MJ, Torkashvand A, Anvari P, Yaseri M. A randomized clinical trial to evaluate the usefulness of amniotic membrane transplantation in bacterial keratitis healing. *Ocul Surf*. 2017;15:218-226.
12. Tandon R, Gupta N, Kalaivani M, Sharma N, Titiyal JS, Vajpayee RB. Amniotic membrane transplantation as an adjunct to medical therapy in acute ocular burns. *Br J Ophthalmol*. 2011;95:199-204.
13. Niknejad H, Peirovi H, Jorjani M, Ahmadiani A, Ghanavi J, Seifalian AM. Properties of the amniotic membrane for potential use in tissue engineering. *Eur Cells Mater*. 2008;15:88-99.
14. Tseng SC, Li DQ, Ma X. Suppression of transforming growth factor-beta isoforms, TGF-beta receptor type II, and myofibroblast differentiation in cultured human corneal and limbal fibroblasts by amniotic membrane matrix. *J Cell Physiol*. 1999;179:325-335.
15. Lee SB, Li DQ, Tan DT, Meller DC, Tseng SC. Suppression of TGF-beta signaling in both normal conjunctival fibroblasts and pterygial body fibroblasts by amniotic membrane. *Curr Eye Res*. 2000;20:325-334.
16. Hao Y, Ma DH, Hwang DG, Kim WS, Zhang F. Identification of anti-angiogenic and antiinflammatory proteins in human amniotic membrane. *Cornea*. 2000;19:348-352.
17. Mamede AC, Botelho MF. In: Mamede AC, Botelho MF, eds. *Amniotic Membrane: Origin, Characterization and Medical Applications*. Springer; 2015.
18. Tehrani FA, Peirovi H, Niknejad H. Determination of antibacterial effect of the epithelial and mesenchymal surfaces of amniotic membrane on *Escherichia coli*, *Staphylococcus aureus*, and *Pseudomonas aeruginosa*. *Qom Univ Med Sci J*. 2013;7:12-22.
19. Kjaergaard N, Hein M, Hyttel L, et al. Antibacterial properties of human amnion and chorion in vitro. *Eur J Obstet Gynecol Reprod Biol*. 2001;94:224-229.
20. Kjaergaard N, Helmgj RB, Schonheyder HC, Ulbjerg N, Hansen ES, Madsen H. Chorioamniotic membranes constitute a competent barrier to group b streptococcus in vitro. *Eur J Obstet Gynecol Reprod Biol*. 1999;83:165-169.
21. Inge E, Talmi YP, Sigler L, Finkelstein Y, Zohar Y. Antibacterial properties of human amniotic membranes. *Placenta*. 1991;12:285-288.
22. Sangwan VS, Basu S. Antimicrobial properties of amniotic membrane. *Br J Ophthalmol*. 2011;95:1-2.
23. Dua HS, Gomes JA, King AJ, Maharajan VS. The amniotic membrane in ophthalmology. *Surv Ophthalmol*. 2004;49:51-77.
24. Shimmura S, Shimazaki J, Ohashi Y, Tsubota K. Antiinflammatory effects of amniotic membrane transplantation in ocular surface disorders. *Cornea*. 2001;20:408-413.
25. Hu DJ, Basti A, Wen A, Bryar PJ. Prospective comparison of corneal re-epithelialization over the stromal and basement membrane surfaces of preserved human amniotic membrane. *ARVO Annual Meeting Abstract*. 2003;22:37-40.
26. Seitz B, Resch MD, Schlötzer-Schrehardt U, Hofmann-Rummelt C, Sauer R, Kruse FE. Histopathology and ultrastructure of human corneas after amniotic membrane transplantation. *Arch Ophthalmol*. 2006;124:1487-1490.
27. von Versen-Höynck F, Syring C, Bachmann S, Möller DE. The influence of different preservation and sterilization steps on the histological properties of amnion allografts—light and scanning electron microscopic studies. *Cell Tissue Bank*. 2004;5:45-56.
28. Lim LS, Poh RW, Riau AK, Beuerman RW, Tan D, Mehta JS. Biological and ultrastructural properties of acelagraft, a freeze-dried γ -irradiated human amniotic membrane. *Arch Ophthalmol*. 2010;128:1303-1310.
29. Tehrani FD, Firouzeh A, Shabani I, Shabani A. A review on modifications of amniotic membrane for biomedical applications. *Front Bioeng Biotechnol*. 2021;13(8):606982.
30. Gholipourmalekabadi M, Mozafari M, Salehi M, et al. Development of a cost-effective and simple protocol for decellularization and preservation of human amniotic membrane as a soft tissue replacement and delivery system for bone marrow stromal cells. *Adv Healthc Mater*. 2015;4:918-926.
31. Keane TJ, Londono R, Turner NJ, Badyak SF. Consequences of ineffective decellularization of biologic scaffolds on the host response. *Biomaterials*. 2012;33:1771-1781.
32. Seif-Naraghi SB, Singelyn JM, Salvatore MA, et al. Safety and efficacy of an injectable extracellular matrix hydrogel for treating myocardial infarction. *Sci Transl Med*. 2013;5:173ra25.
33. Aamodt JM, Grainger DW. Extracellular matrix-based biomaterial scaffolds and the host response. *Biomaterials*. 2016;86:68-82.
34. Balestrini JL, Gard AL, Liu A, et al. Production of decellularized porcine lung scaffolds for use in tissue engineering. *Integr Biol (Camb)*. 2015;7:1598-1610.
35. Bhatia M, Pereira M, Rana H, et al. The mechanism of cell interaction and response on decellularized human amniotic membrane: implications in wound healing. *Wounds*. 2007;19:207-217.
36. Rodríguez-Ares MT, López-Valladares MJ, Touriño R, et al. Effects of lyophilization on human amniotic membrane. *Acta Ophthalmol*. 2009;87:396-403.
37. Mao Y, John N, Protzman NM, et al. A decellularized flowable placental connective tissue matrix supports cellular functions of human tenocytes in vitro. *J Exp Orthop*. 2022;9(1):69.
38. Mao Y, Jacob V, Singal A, Lei S, Park MS, Lima MRN, Li C, Dhall S, Sathyamoorthy M, Kohn J. Exosomes secreted from amniotic membrane contribute to its anti-fibrotic activity. *Int J Mol Sci*. 2021;22.
39. Mao Y, Hoffman T, Wu A, Goyal R, Kohn J. Cell type-specific extracellular matrix guided the differentiation of human mesenchymal stem cells in 3d polymeric scaffolds. *J Mater Sci Mater Med*. 2017;28:100.
40. Rho CR, Park MY, Kang S. Effects of granulocyte-macrophage colony-stimulating (GM-CSF) factor on corneal epithelial cells in corneal wound healing model. *PLoS One*. 2015;10:e0138020.
41. Hafezi F, Gatziofous Z, Angunawela R, Ittner LM. Absence of IL-6 prevents corneal wound healing after deep excimer laser ablation in vivo. *Eye (Lond)*. 2018;32:156-157.
42. Arranz-Valsero I, Soriano-Romani L, García-Posadas L, López-García A, Diebold Y. IL-6 as a corneal wound healing mediator in an in vitro scratch assay. *Exp Eye Res*. 2014;125:183-192.
43. Ebihara N, Matsuda A, Nakamura S, Matsuda H, Murakami A. Role of the IL-6 classic- and trans-signaling pathways in corneal sterile inflammation and wound healing. *Invest Ophthalmol Vis Sci*. 2011;52:8549-8557.

44. Nishida T, Nakamura M, Mishima H, Otori T, Hikida M. Interleukin 6 facilitates corneal epithelial wound closure in vivo. *Arch Ophthalmol*. 1992;110:1292-1294.
45. Strieter RM, Kunkel SL, Eliner VM, et al. Interleukin-8. A corneal factor that induces neovascularization. *Am J Pathol*. 1992;141:1279-1284.
46. Koch AE, Polverini PJ, Kunkel SL, et al. Interleukin-8 as a macrophage-derived mediator of angiogenesis. *Science*. 1992;258:1798-1801.
47. Wang X, Zhang S, Dong M, Li Y, Zhou Q, Yang L. The proinflammatory cytokines IL-1 β and TNF- α modulate corneal epithelial wound healing through p16Ink4a suppressing STAT3 activity. *J Cell Physiol*. 2020;235:10081-10093.
48. Yang L, Zhang S, Duan H, et al. Different effects of pro-inflammatory factors and hyperosmotic stress on corneal epithelial stem/progenitor cells and wound healing in mice. *Stem Cells Transl Med*. 2019;8:46-57.
49. Keene DR, Sakai LY, Lunstrum GP, Morris NP, Burgeson RE. Type VII collagen forms an extended network of anchoring fibrils. *J Cell Biol*. 1987;104:611-621.
50. Sonnenberg A, Calafat J, Janssen H, et al. Integrin alpha 6/beta 4 complex is located in hemidesmosomes, suggesting a major role in epidermal cell-basement membrane adhesion. *J Cell Biol*. 1991;113(4):907-917.
51. Terranova VP, Lyall RM. Chemotaxis of human gingival epithelial cells to laminin. A mechanism for epithelial cell apical migration. *J Periodontol*. 1986;57(5):311-317.
52. Kurpakus MA, Stock EL, Jones JC. The role of the basement membrane in differential expression of keratin proteins in epithelial cells. *Dev Biol*. 1992;150:243-255.
53. Streuli CH, Bailey N, Bissell MJ. Control of mammary epithelial differentiation: basement membrane induces tissue-specific gene expression in the absence of cell-cell interaction and morphological polarity. *J Cell Biol*. 1991;115:1383-1395.
54. Guo M, Grinnell F. Basement membrane and human epidermal differentiation in vitro. *J Invest Dermatol*. 1989;93:372-378.
55. Boudreau N, Werb Z, Bissell MJ. Suppression of apoptosis by basement membrane requires three-dimensional tissue organization and withdrawal from the cell cycle. *Proc Natl Acad Sci U S A*. 1996;93:3509-3513.
56. Boudreau N, Simpson CJ, Werb Z, Bissell MJ. Suppression of ICE and apoptosis in mammary epithelial cells by extracellular matrix. *Science*. 1995;267:891-893.
57. Kruse FE, Jousen AM, Rohrschneider K, et al. Cryopreserved human amniotic membrane for ocular surface reconstruction. *Graefes Arch Clin Exp Ophthalmol*. 2000;238:68-75.
58. Kubo M, Sonoda Y, Muramatsu R, Usui M. Immunogenicity of human amniotic membrane in experimental xenotransplantation. *Invest Ophthalmol Vis Sci*. 2001;42:1539-1546.
59. Chuck RS, Graff JM, Bryant MR, Sweet PM. Biomechanical characterization of human amniotic membrane preparations for ocular surface reconstruction. *Ophthalmic Res*. 2004;36:341-348.
60. Koizumi N, Fullwood NJ, Bairaktaris G, Inatomi T, Kinoshita S, Quantock AJ. Cultivation of corneal epithelial cells on intact and denuded human amniotic membrane. *Invest Ophthalmol Vis Sci*. 2000;41:2506-2513.
61. Sosnová-Netuková M, Kuchynka P, Forrester JV. The suprabasal layer of corneal epithelial cells represents the major barrier site to the passive movement of small molecules and trafficking leukocytes. *Br J Ophthalmol*. 2007;91:372-378.
62. Kumar V, Abbas AK, Aster JC. Cell injury, cell death, and adaptations. In: Kumar V, Abbas AK, Aster JC, eds. *Robins Basic Pathology*. Elsevier Saunders; 2013:1-28.
63. Solomon A, Rosenblatt M, Monroy D, Ji Z, Pflugfelder SC, Tseng SC. Suppression of interleukin 1 alpha and interleukin 1 beta in the human limbal epithelial cells cultured on the amniotic membrane stromal matrix. *Br J Ophthalmol*. 2001;85:444-449.
64. van Nieuwenhuijze A, Koenders M, Roeleveld D, Sleeman MA, van den Berg W, Wicks IP. GM-CSF as a therapeutic target in inflammatory diseases. *Mol Immunol*. 2013;56:675-682.
65. Parmiani G, Castelli C, Pilla L, Santinami M, Colombo MP, Rivoltini L. Opposite immune functions of GM-CSF administered as vaccine adjuvant in cancer patients. *Ann Oncol*. 2007;18:226-232.
66. Bhattacharya P, Budnick I, Singh M, et al. Dual role of GM-CSF as a pro-inflammatory and a regulatory cytokine: implications for immune therapy. *J Interferon Cytokine Res*. 2015;35:585-599.
67. Shachar I, Karin N. The dual roles of inflammatory cytokines and chemokines in the regulation of autoimmune diseases and their clinical implications. *J Leukoc Biol*. 2013;93:51-61.
68. Sangwan VS, Basu S, MacNeil S, Balasubramanian D. Simple limbal epithelial transplantation (SLET): a novel surgical technique for the treatment of unilateral limbal stem cell deficiency. *Br J Ophthalmol*. 2012;96(7):931-934.
69. Maharajan VS, Shanmuganathan V, Currie A, Hopkinson A, Powell-Richards A, Dua HS. Amniotic membrane transplantation for ocular surface reconstruction: indications and outcomes. *Clin Experiment Ophthalmol*. 2007;35:140-147.
70. Röck T, Bramkamp M, Bartz-Schmidt KU, Röck D. A retrospective study to compare the recurrence rate after treatment of pterygium by conjunctival autograft, primary closure, and amniotic membrane transplantation. *Med Sci Monit*. 2019;25:7976-7981.
71. Akbari M, Soltani-Moghadam R, Elmi R, Kazemnejad E. Comparison of free conjunctival autograft versus amniotic membrane transplantation for pterygium surgery. *J Curr Ophthalmol*. 2017;29:282-286.
72. Rama P, Matuska S, Paganoni G, Spinelli A, De Luca M, Pellegrini G. Limbal stem-cell therapy and long-term corneal regeneration. *N Engl J Med*. 2010;363:147-155.
73. Shortt AJ, Secker GA, Lomas RJ, et al. The effect of amniotic membrane preparation method on its ability to serve as a substrate for the ex-vivo expansion of limbal epithelial cells. *Biomaterials*. 2009;30:1056-1065.
74. Sheha H, Kheirkhah A, Taha H. Amniotic membrane transplantation in trabeculectomy with mitomycin C for refractory glaucoma. *J Glaucoma*. 2008;17:303-307.
75. Agrawal U, Rundle P, Rennie IG, Salvi S. Fresh frozen amniotic membrane for conjunctival reconstruction after excision of neoplastic and presumed neoplastic conjunctival lesions. *Eye (Lond)*. 2017;31:884-889.
76. Hanada K, Shimazaki J, Shimmura S, Tsubota K. Multilayered amniotic membrane transplantation for severe ulceration of the cornea and sclera. *Am J Ophthalmol*. 2001;131:324-331.
77. Ma DH, Wang SF, Su WY, Tsai RJ. Amniotic membrane graft for the management of scleral melting and corneal perforation in recalcitrant infectious scleral and corneoscleral ulcers. *Cornea*. 2002;21:275-283.
78. Fenelon M, Maurel DB, Siadous R, et al. Comparison of the impact of preservation methods on amniotic membrane properties for tissue engineering applications. *Mat Sci Eng C*. 2019;104:109903.
79. Salah RA, Mohamed IK, El-Badri N. Development of decellularized amniotic membrane as a bioscaffold for bone marrow-derived mesenchymal stem cells: ultrastructural study. *J Mol Histol*. 2018;49:289-301.
80. Gholipourmalekabadi M, Sameni M, Radenkovic D, Mozafari M, Mossahebi-Mohammadi M, Seifalian A. Decellularized human amniotic membrane: how viable is it as a delivery system for human adipose tissue-derived stromal cells? *Cell Prolif*. 2016;49:115-121.
81. Taghiabadi E, Nasri S, Shafieyan S, Firoozinezhad SJ, Aghdami N. Fabrication and characterization of spongy denuded amniotic membrane based scaffold for tissue engineering. *Cell J*. 2015;16:476-487.
82. Francisco JC, Correa Cunha R, Cardoso MA, et al. Decellularized amniotic membrane scaffold as a pericardial substitute: An in vivo study. *Transplant Proc*. 2016;48:2845-2849.

83. Kassem RR, El-Mofty RMA, Khodeir MM, Hamza WM. A comparative study of different amniotic membrane orientations during extraocular muscle surgery in rabbits. *Curr Eye Res.* 2018;43(3):325-332.
84. Kennedy JB, Larochelle MB, Pedler MG, Petrash JM, Enzenauer RW. The effect of amniotic membrane grafting on healing and wound strength after strabismus surgery in a rabbit model. *J AAPOS.* 2018; 22(1):22-26.e1.
85. Chun BY, Kim HK, Shin JP. Dried human amniotic membrane does not alleviate inflammation and fibrosis in experimental strabismus surgery. *J Ophthalmol.* 2013;2013:369126.
86. Kassem RR, Khodeir MM, Salem M, et al. Effect of cryopreserved amniotic membrane on the development of adhesions and fibrosis after extraocular muscle surgery in rabbits. *Acta Ophthalmol.* 2013; 91(2):e140-e148.
87. Kassem RR, Abdel-Hamid MA, Khodeir MM. Effect of lyophilized amniotic membrane on the development of adhesions and fibrosis after extraocular muscle surgery in rabbits. *Curr Eye Res.* 2011;36(11): 1020-1027.
88. Mehendale RA, Dagi LR. Amniotic membrane implantation to reduce extraocular muscle adhesions to a titanium implant. *J AAPOS.* 2011; 15(4):404-406.
89. Kassem RR, El-Mofty RMA. Amniotic membrane transplantation in strabismus surgery. *Curr Eye Res.* 2019;44(5):451-464.
90. Kassem RR, Gawdat GI, Zedan RH. Severe fibrosis of extraocular muscles after the use of lyophilized amniotic membrane in strabismus surgery. *J AAPOS.* 2010;14:548-549.
91. Hovanesian JA. History of amniotic membranes in pterygium surgery. In: Hovanesian JA, ed. *Pterygium: Techniques and Technologies for Surgical Success.* SLACK Incorporated; 2012:65-75.
92. Memarzadeh F, Fahd AK, Shamie N, Chuck RS. Comparison of de-epithelialized amniotic membrane transplantation and conjunctival autograft after primary pterygium excision. *Eye (Lond).* 2008;22:107-112.

SUPPORTING INFORMATION

Additional supporting information can be found online in the Supporting Information section at the end of this article.

How to cite this article: Mao Y, Protzman NM, John N, et al. An in vitro comparison of human corneal epithelial cell activity and inflammatory response on differently designed ocular amniotic membranes and a clinical case study. *J Biomed Mater Res.* 2022;1-17. doi:[10.1002/jbm.b.35186](https://doi.org/10.1002/jbm.b.35186)